

Dynamic mechanical measurement of the viscoelasticity of single adherent cells

Elise A. Corbin, Olaoluwa O. Adeniba, Randy H. Ewoldt, and Rashid Bashir

Citation: [Applied Physics Letters](#) **108**, 093701 (2016); doi: 10.1063/1.4942364

View online: <http://dx.doi.org/10.1063/1.4942364>

View Table of Contents: <http://scitation.aip.org/content/aip/journal/apl/108/9?ver=pdfcov>

Published by the [AIP Publishing](#)

Articles you may be interested in

[Highly selective biomechanical separation of cancer cells from leukocytes using microfluidic ratchets and hydrodynamic concentrator](#)

[Biomicrofluidics](#) **7**, 034114 (2013); 10.1063/1.4812688

[Label-free isolation of circulating tumor cells in microfluidic devices: Current research and perspectives](#)

[Biomicrofluidics](#) **7**, 011810 (2013); 10.1063/1.4780062

[Probing the mechanical properties of brain cancer cells using a microfluidic cell squeezer device](#)

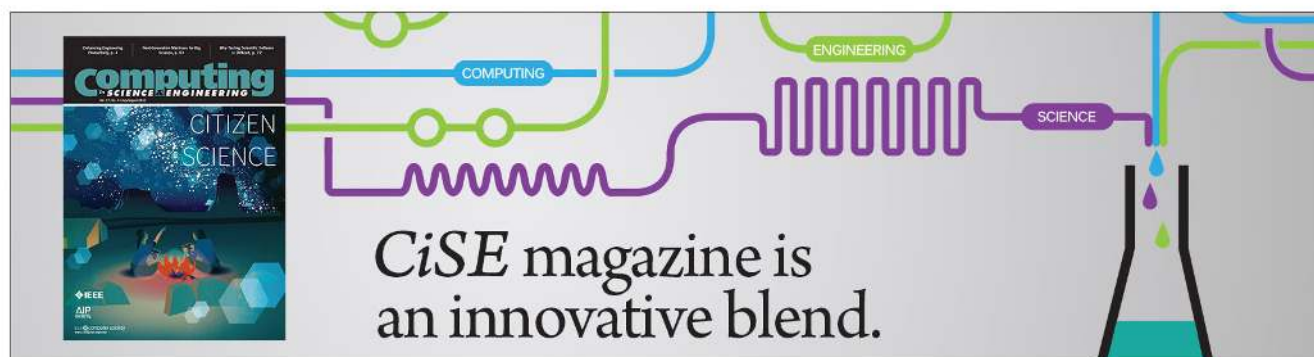
[Biomicrofluidics](#) **7**, 011806 (2013); 10.1063/1.4774310

[Rapid isolation of cancer cells using microfluidic deterministic lateral displacement structure](#)

[Biomicrofluidics](#) **7**, 011801 (2013); 10.1063/1.4774308

[Selective cell capture and analysis using shallow antibody-coated microchannels](#)

[Biomicrofluidics](#) **6**, 044117 (2012); 10.1063/1.4771968



Dynamic mechanical measurement of the viscoelasticity of single adherent cells

Elise A. Corbin,^{1,2,a)} Olaoluwa O. Adeniba,^{2,3,a)} Randy H. Ewoldt,³ and Rashid Bashir^{1,2,b)}

¹Department of Bioengineering, University of Illinois Urbana-Champaign, Urbana, Illinois 61801, USA

²Micro and Nanotechnology Laboratory, University of Illinois Urbana-Champaign, Urbana, Illinois 61801, USA

³Department of Mechanical Science and Engineering, University of Illinois Urbana-Champaign, Urbana, Illinois 61801, USA

(Received 30 October 2015; accepted 2 February 2016; published online 4 March 2016)

Many recent studies on the viscoelasticity of individual cells link mechanics with cellular function and health. Here, we introduce a measurement of the viscoelastic properties of individual human colon cancer cells (HT-29) using silicon pedestal microelectromechanical systems (MEMS) resonant sensors. We demonstrate that the viscoelastic properties of single adherent cells can be extracted by measuring a difference in vibrational amplitude of our resonant sensor platform. The magnitude of vibration of the pedestal sensor is measured using a laser Doppler vibrometer (LDV). A change in amplitude of the sensor, compared with the driving amplitude (amplitude ratio), is influenced by the mechanical properties of the adhered cells. The amplitude ratio of the fixed cells was greater than the live cells, with a p -value < 0.0001 . By combining the amplitude shift with the resonant frequency shift measure, we determined the elastic modulus and viscosity values of 100 Pa and 0.0031 Pa s, respectively. Our method using the change in amplitude of resonant MEMS devices can enable the determination of a refined solution space and could improve measuring the stiffness of cells. © 2016 AIP Publishing LLC. [<http://dx.doi.org/10.1063/1.4942364>]

Understanding and defining the mechanical properties of cells and tissues as a biomarker has become a nexus of next generation disease diagnostics. Recently, the development of more precise, reliable, and versatile measurement techniques—such as atomic force microscopy (AFM),^{1–3} magnetic twisting cytometry,⁴ micropipette aspiration,^{5–7} optomechanical measures,⁸ and quartz crystal microbalance (QCM)⁹—have provided a greater understanding of how the physical properties of a cell affect its behavior in disease. Viscoelastic properties have been linked to diseases such as cancer, where cancer cells are less stiff than their normal counterparts. These mechanical properties of cancer cells could be useful biomarkers⁵ for evaluating cycle progression, cellular physiology, and metabolism that underpin the characteristics of cancer. However, there are many limitations to the current state of the art measurements (see supplementary material¹⁰). Micropipette aspiration uses a flow-through configuration that allows for high throughput, but limits the types of cells for investigation to cells in suspension. Although QCM and AFM can study adherent cells, their sample sizes are limited based on electrode dimensions or data analysis complicated by intricate tip geometry, respectively.

This work reports a vibration-based measurement technique used to characterize the viscoelasticity of individual adherent colon cancer (HT-29) cells. Previously, we quantified differences between live and fixed cells using microelectromechanical systems (MEMS) resonant sensors and the viscoelastic effect on the resonant frequency of the sensor. In this study, we demonstrate the use of these resonant sensors to investigate the viscoelasticity of single adherent cells by

instead exploring the vibration amplitude effects. Analytical modeling shows that loading the sensor with a viscoelastic material, as opposed to an infinitely stiff point mass, results in a decreased vibration amplitude at resonance. Experimentally we compare live and fixed cells, where fixed cells, known to have a higher stiffness, exhibit behavior closer to a point mass than the live counterparts and therefore show a smaller amplitude effect. Combining the frequency shift reported previously¹¹ and the amplitude change reported here, we can more concretely determine the viscoelastic properties of the cell.

The MEMS resonant sensor structure used in this work comprises a $60 \times 60 \mu\text{m}^2$ platform suspended by four beam springs that are arrayed in a 9×9 format of 81 sensors. The sensors operate in the first mode with the aid of electromagnetic stimulation generating Lorentz force actuation. Figure 1(a) shows a schematic of a single cell vibrating on the sensor where we compare the driving amplitude of the sensor with the amplitude response of the sensor loaded with a cell. In this case, the cell is presented as an added mass Kelvin–Voigt viscoelastic solid, where the material behavior is considered as that of a spring and damper in parallel. Similar to the previous studies,^{11–13} the velocity of the sensor vibration is monitored and measured by a laser Doppler vibrometer (LDV) in conjunction with a lock-in amplifier to capture a resonant frequency shift (see supplementary material¹⁰). In this work, we also capture the vibration amplitude response after finding the device resonance.

To observe significant changes in vibrational amplitude of the pedestal, we must consider the dominant forces governing the vibration of the sensor and the cell to ensure that these experimental conditions are appropriate to capture viscoelastic effects. Figure 1(b) shows three case scenarios in which the cell height is compared with a elastic shear

^{a)}E. A. Corbin and O. O. Adeniba contributed equally to this work.

^{b)}rbashir@illinois.edu

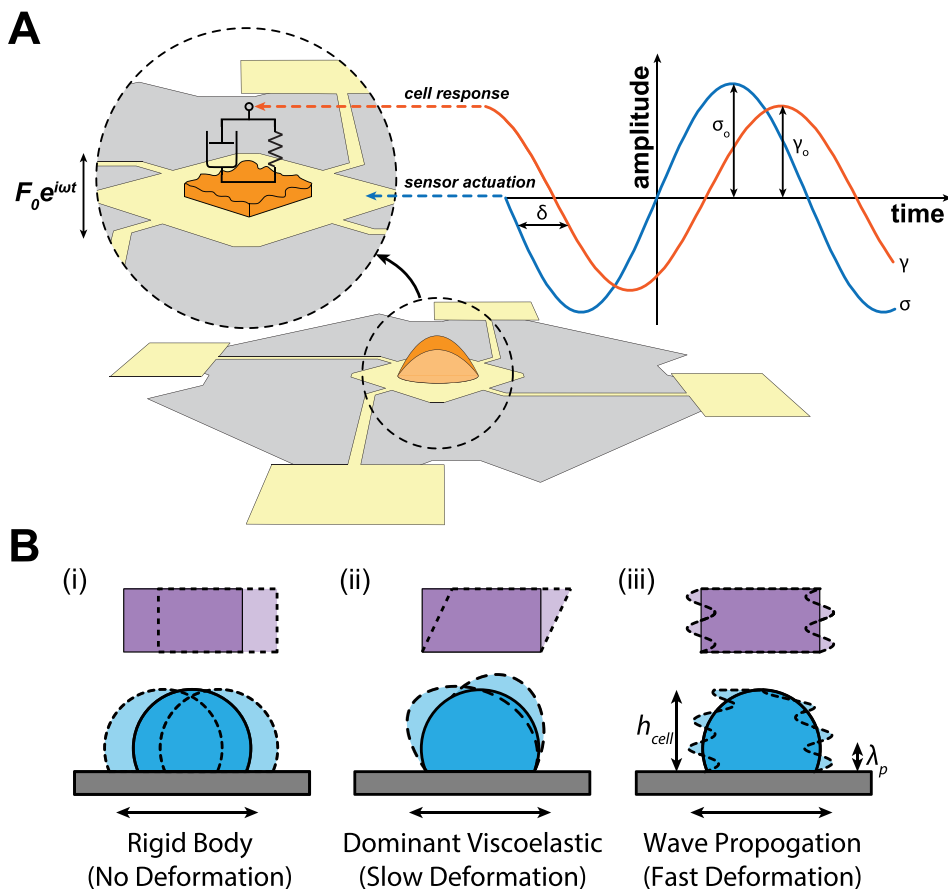


FIG. 1. Experimental overview. (a) Schematic of the vibration of a cell as a Kelvin–Voigt viscoelastic solid on the sensor describing the excitation ($F_0 e^{i\omega t}$) and cell amplitude response. Stress (σ_0) and induced strain (γ_0) related to the applied force and cell response, respectively. (b) Schematic diagram showing the possible scenarios of dominant forces that operate in the regime of vibration: (i) Cell is a rigid body and only translates; (ii) Cell slowly deforms because the height of the cell, h_{cell} , is shorter than the wavelength of elastic wave propagation, λ_p ; (iii) Elastic wave force dominates motion and only propagates fast across cell: $h_{cell} > \lambda_p$.

wave propagation. The cases are as follows: (i) *rigid body*, no deformation; (ii) *dominantly viscoelastic*, $\lambda_p > h_{cell}$, the elastic wavelength is longer than the cell height; and (iii) *elastic wave propagation*, $\lambda_p < h_{cell}$, the elastic wavelength is shorter than the cell height. We compare the cell height, h_{cell} , with the wavelength scale estimate of the elastic shear wave propagation, (see supplementary material¹⁰). Consideration of a shear force acting on the sensor is sufficient for a tractable cell deformation analysis. We can conclude that the dominant forces in our system are such to produce observable viscoelastic effects.

For this work, we consider the ratio of the amplitude of a cell-filled sensor to that of the empty (unloaded) sensor. The unloaded sensor is modeled as a one degree of freedom (1-DOF) system, while the loaded sensor is considered in two contrasting scenarios: with the cell being a point mass or a viscoelastic solid (Figure 2(a)). As in previous works, we model the viscoelastic cell as a Kelvin–Voigt solid¹⁴ and the entire system of the viscoelastic solid adhered to the sensor is modeled as a two degree of freedom (2-DOF) spring-mass-damper dynamic system. To elucidate the effect of the viscoelasticity of the cell on the amplitude, the ratio of the apparent amplitude (2-DOF) to the applied amplitude (1-DOF) was calculated over a wide range of elastic moduli and viscosities of cells (Figure 2(b)). The shape of the model clearly shows that the viscoelastic parameters affect the amplitude ratio, with areas of very strong effects, similar to the frequency response previously investigated.^{11–13} We illustrate this effect in Figure 2(c) by simulating the response across the frequency spectrum for both low and high viscoelastic mass loaded sensors. The inset of Figure 2(c) more

clearly portrays the drop in amplitude with changing viscoelastic parameters as compared with an empty sensor, where the amplitude decrease of the low viscoelastic case is much larger with respect to the reference, than the high viscoelastic case.

To investigate the amplitude effects experimentally, human colon adenocarcinoma cells (HT-29) were cultured on the resonant sensors functionalized with collagen similar to earlier studies.¹¹ Briefly, HT-29 cells were grown at 37 °C in Dulbecco’s Modified Eagle Medium (DMEM) supplemented with sodium pyruvate, 10% fetal bovine serum (FBS), and 1% penicillin streptomycin. Cells were seeded onto the sensor area at a density of ~ 300 cell/mm² within a 6 mm diameter polydimethylsiloxane (PDMS) culture chamber. After measuring the amplitude of the resonant peak with a live cell attached to the sensor, the cells were then fixed with 4% paraformaldehyde for 30 min, which has been shown to increase stiffness with minimal volumetric decrease.^{15,16}

Our measurement scheme consists of measuring the amplitude of the sensor three times: empty, then loaded with a live cell, and then after the same cell is fixed. Throughout the measurement, there is an observed amplitude drift, which was corrected by monitoring the resonant amplitude of nearby sensors without the captured cells (see supplementary material¹⁰). Figure 2(d) presents the changes in amplitude between an empty reference sensor, the same sensor loaded with a live cell, and the same sensor and cell after fixation. The experimental results showed that live cells, which are less stiff, depict a greater amplitude difference relative to the reference sensor. When the stiffness of the cell was increased

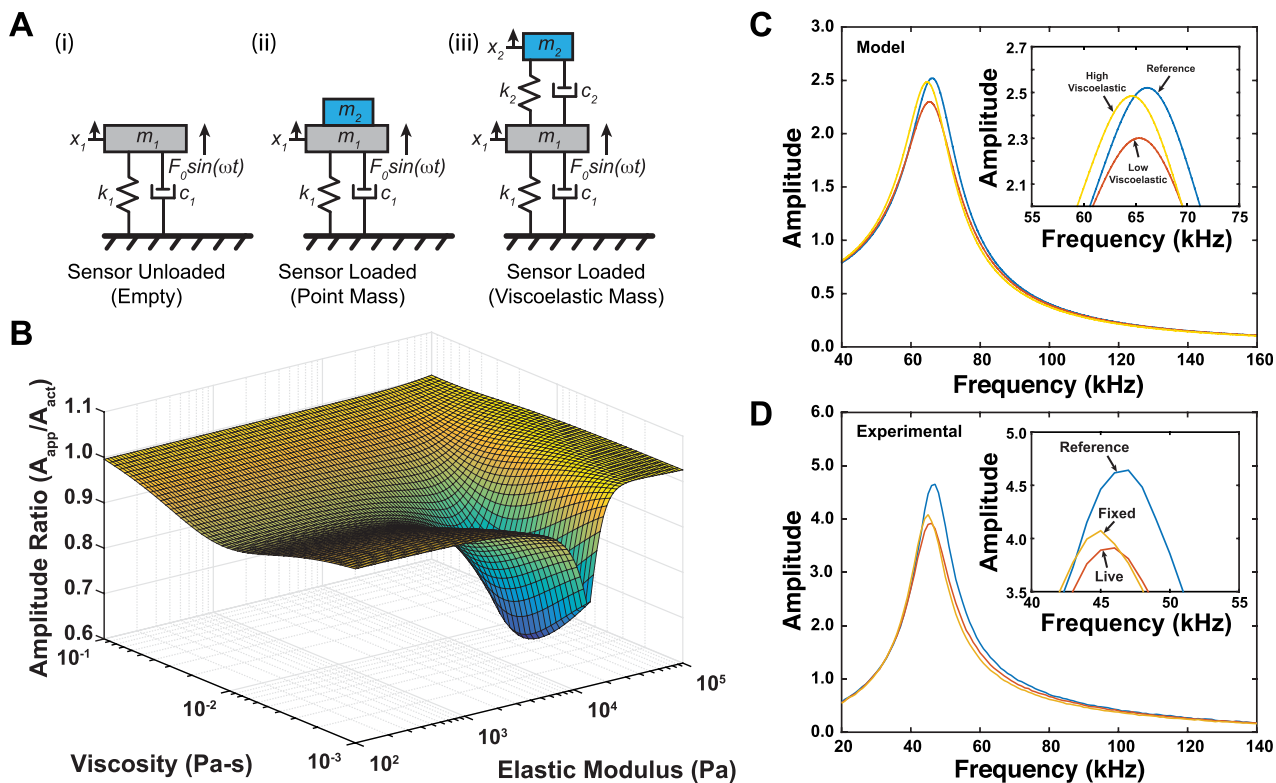


FIG. 2. (a) Schematics of a Kelvin-Voigt viscoelastic solid model system: (i) a 1DOF representing the model of an unloaded sensor, (ii) a 2-DOF dynamical sensor-cell model demonstrating a conventional mass-spring-damper system, and (iii) an improved mass-spring-damper 2-DOF system used to obtain the vibrational amplitude and frequency from experimental data. (b) A three-dimensional surface plot depicting how cell viscoelasticity (elastic modulus and viscosity) affects amplitude ratio (amplitude ratio is apparent amplitude divided by actual amplitude). (c)–(d) Frequency spectra of the viscoelastic response of (c) model viscoelastic solid and (d) HT-29 cell; Insets: highlight the shift in amplitude.

through fixation, the amplitude increased as well, agreeing well with our model (Figure 2(c)).

Figure 3(a) shows the amplitude ratio comparison between both live and fixed values of all cells investigated in this study ($n = 16$). There is a consistent increase in the amplitude ratio of the fixed cell compared with the live cell. Again, the amplitude ratio for both live and fixed cells is defined as the amplitude of a cell-loaded sensor (live or fixed) to the amplitude of a reference (empty) sensor. We further illustrate the amplitude differences for each cell by plotting the live amplitude ratio against the fixed amplitude ratio (Figure 3(b)) and comparing with a slope of unity (dotted line). The inset of Figure 3(b) shows a histogram of the difference of the live and fixed ratios for each cell and a normal distribution fit (dotted line) to the data, compared with a normal distribution centered at zero. A paired t-test confirmed the significance of the observed differences before and after fixation (p -value < 0.0001). Paraformaldehyde is known to increase the stiffness of a cell and, through measurements with AFM, fixed cells exhibit greater viscous behavior.¹² Our experimental findings of increased amplitude with fixation agree with this known increase in cell viscoelasticity.

An additional and complementary viscoelastic effect is the shifting of resonant frequency since the cell is oscillating out of phase with the sensor platform.^{11–13,17} The frequency response with respect to viscoelastic parameters produces a similar yet distinct analytical model shape over a range of elastic moduli and viscosities compared with the amplitude

response (see supplementary material¹⁰). Both amplitude and frequency models contain many solutions to any given measurement, and strategies need to be devised to restrict these solution spaces. In the past, we achieved this by using a range of hydrogel concentrations and assuming a model relationship,¹³ or relied on a population measurement with several different cell sizes.¹² Both approaches require many measurements to approach a solution. However, combining both amplitude and frequency measurements narrows the solutions for individual cells based on the overlapping regions from each measurement.

Figure 4 shows the entire solution space regarding possible viscoelastic properties of cells that could lead to the observed data. To create these plots, we took the measured amplitude and frequency data, calculated the mean and standard deviation, and created probability maps for each expected point based on a normal distribution. The resulting solution sets for both the amplitude space and frequency spaces are presented in Figures 4(a) and 4(b), respectively. The amplitude solutions exist in two distinct regions—one that encompasses low viscoelastic properties and one that includes much stiffer and more viscous materials. Similar behavior occurs from the frequency shift model, but the possible solutions only exist in a single, low viscoelastic region. We multiplied the two probabilities to determine the common solution space in Figure 4(c). Through the use of both measurements, we deduce that the viscoelasticity of the cells resides with the low viscosity low elastic moduli region, which agrees well with previous results.¹⁸ The maximum

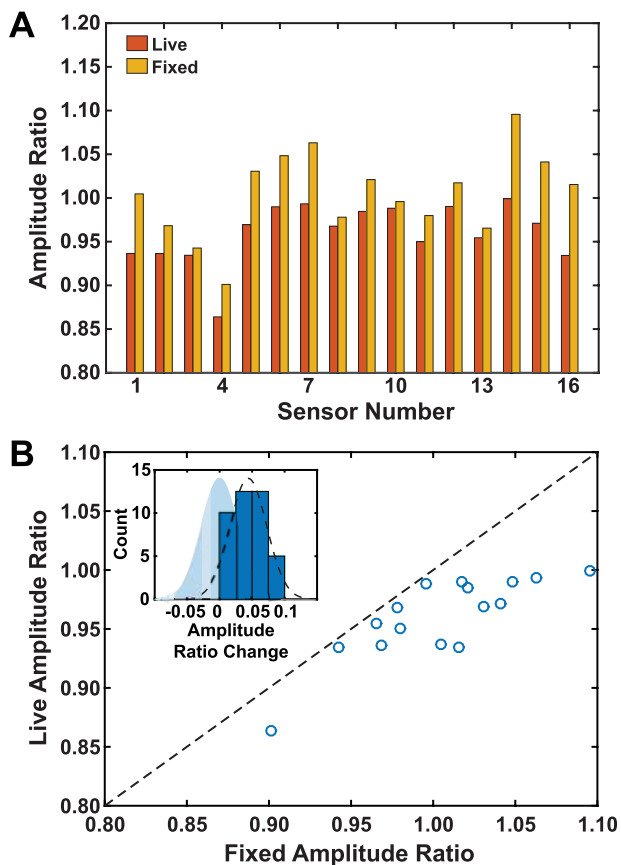


FIG. 3. Experimental results: (a) Bar chart showing an amplitude ratio comparison between both live and fixed values of the same cells. (b) A dotted line of unity slope comparing the plot of live amplitude against fixed amplitude ratios shows a significant difference between the ratio before and after fixation. The inset shows a histogram of the difference of the live and fixed ratios for each cell. A normal distribution (dotted line) is fitted to these data and compared with a standard normal distribution.

probability of this solution states that the elasticity and viscosity values are 100 Pa and 0.0031 Pa s, respectively, at the frequency of measurement.

This work provides a non-destructive method for measuring the viscoelastic properties of cells; however, there are some considerations for future work. Here, we utilized the known size and shape of these cells, in combination with the dark field cross-sectional area of the cell captured during measurement, to estimate each cell size based on a previous work relating the dark field area to the confocal volume.¹¹ This estimation could be improved by incorporating advanced optical imaging capabilities into the LDV system to simultaneously determine the volume, amplitude, and frequency data. Also, the nature of the substrate affects how a cell organizes its cytoskeleton, which in turn influences the effective cell stiffness. The viscoelastic property measurements in this work are limited by the base substrate of the sensor material with a thin surface layer of collagen. Future studies capable of manipulating substrate rigidity, such as deposition of micropatterned hydrogels,^{13,19} could explore the spectrum of cell biomechanics and substrate dependence.

Recently, we have used the same platform to make measurements of cell mechanics in a similar fashion.¹² However, in those works, we took advantage of only the resonant frequency shift that occurs from material

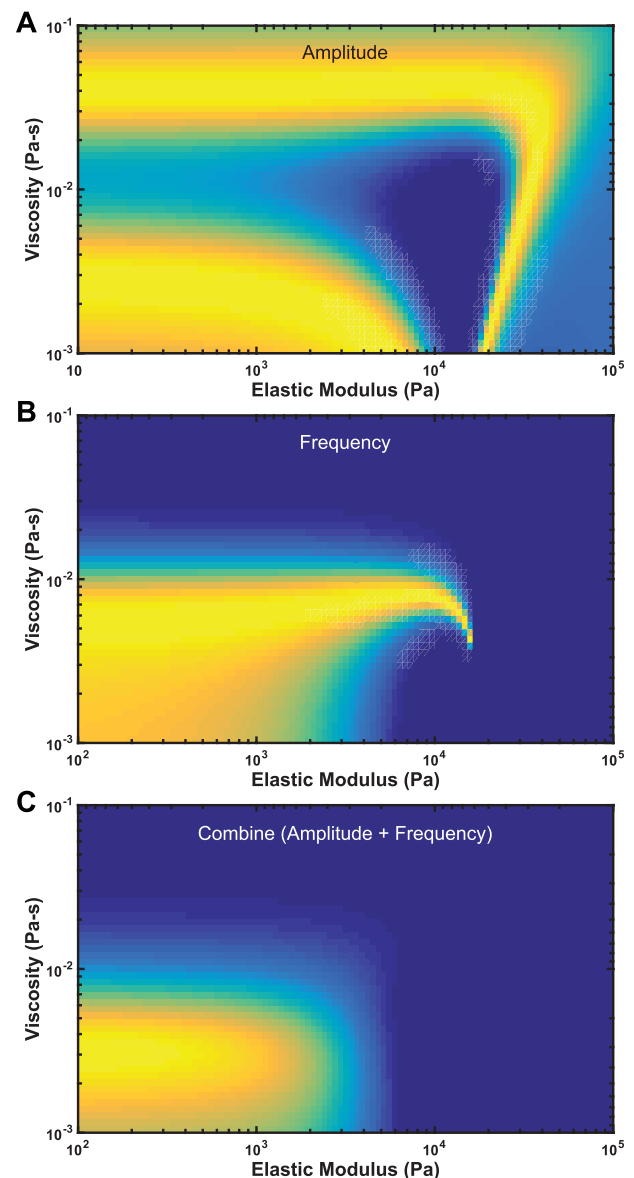


FIG. 4. Potential real solution space (yellow) of viscoelasticity of cells obtained from a normal distribution of observed data. (a) Two distinct regions (yellow) of amplitude solution space. (b) Frequency-shift solution space. (c) Resulting overlapping region of amplitude and frequency-shift solution spaces. The estimated elastic modulus and viscosity from the cell population density is 100 Pa and 0.0031 Pa s, respectively.

viscoelasticity, while in this current work we explored the vibration amplitude dependence on viscoelasticity. This approach is advantageous because it better decouples the material mass from the viscoelastic properties. In this respect, the use of the two independent and complementary measurements can generate more accurate estimates of cell properties from the resonant sensors. Future work will incorporate all of these measurements into cell growth experiments with the resonant sensors for real-time measurement of mass and stiffness over time.

¹T. G. Kuznetsova, M. N. Starodubtseva, N. I. Yegorenkov, S. A. Chizhik, and R. I. Zhdanov, *Micron* **38**, 824 (2007).

²S. E. Cross, Y.-S. Jin, J. Rao, and J. K. Gimzewski, *Nat. Nano* **2**, 780 (2007).

- ³M. Plodinec, M. Loparic, C. A. Monnier, E. C. Obermann, R. Zanetti-Dallenbach, P. Oertle, J. T. Hyotyla, U. Aebi, M. Bentires-Alj, R. Y. H. Lim, and C.-A. Schoenenberger, *Nat. Nano* **7**, 757 (2012).
- ⁴N. Wang, J. P. Butler, and D. E. Ingber, *Science* **260**, 1124 (1993).
- ⁵R. M. Hochmuth, *J. Biomech.* **33**, 15 (2000).
- ⁶M. Sato, N. Ohshima, and R. M. Nerem, *J. Biomech.* **29**, 461 (1996).
- ⁷A. Y. E. Evans, *Biophys. J.* **56**, 151 (1989).
- ⁸K. Park, A. Mehrnezhad, E. A. Corbin, and R. Bashir, *Lab Chip* **15**, 3460 (2015).
- ⁹J. Li, C. Thielemann, U. Reuning, and D. Johannsmann, *Biosens. Bioelectron.* **20**, 1333 (2005).
- ¹⁰See supplementary material at <http://dx.doi.org/10.1063/1.4942364> for device operation and amplitude measurement, mechanical model dynamics, viscoelastic state determination, system linearization, and viscoelastic method comparison.
- ¹¹K. Park, L. J. Millet, N. Kim, H. Li, X. Jin, G. Popescu, N. R. Aluru, K. J. Hsia, and R. Bashir, *Proc. Natl. Acad. Sci. U. S. A.* **107**, 20691 (2010).
- ¹²E. A. Corbin, F. Kong, C. T. Lim, W. P. King, and R. Bashir, *Lab Chip* **15**, 839 (2015).
- ¹³E. A. Corbin, L. J. Millet, J. H. Pikul, C. L. Johnson, J. G. Georgiadis, W. P. King, and R. Bashir, *Biomed. Microdevices* **15**, 311 (2013).
- ¹⁴Y.-C. Fung, *Biomechanics: Mechanical Properties of Living Tissues* (Springer-Verlag, New York, 1981).
- ¹⁵F. Braet, C. Rotsch, E. Wisse, and M. Radmacher, *Appl. Phys. A: Mater.* **66**, S575 (1998).
- ¹⁶J. Hutter, J. Chen, W. Wan, S. Uniyal, M. Leabu, and B. Chan, *J. Microsc. (Oxford)* **219**, 61 (2005).
- ¹⁷E. A. Corbin, L. J. Millet, K. R. Keller, W. P. King, and R. Bashir, *Anal. Chem.* **86**, 4864 (2014).
- ¹⁸M. Abdollahad, S. Mohajerzadeh, M. Janmaleki, H. Taghinejad, and M. Taghinejad, *Integr. Biol.* **5**, 535 (2013).
- ¹⁹E. A. Corbin, B. R. Dorvel, L. J. Millet, W. P. King, and R. Bashir, *Lab Chip* **14**, 1401 (2014).